Design Optimization of a HOM Absorber for the Cornell ERL

Elise Novitski
Physics Department, Yale University, New Haven, CT, 06520
(Dated: September 24, 2006)

CLANS and Microwave Studio computer models were used to investigate the effects of changes in the design of the higher-order mode load for the proposed Cornell Energy Recovery Linac. Changes in thickness and in the radial position of plates of lossy materials were shown to substantially affect $\frac{R_0}{Q_0}Q$ of high-Q HOMs and may therefore be useful as optimization parameters, while changing the length of the tube between the cavity and the load and changing the length of the lossy materials in the load were shown to be have weaker effects on $\frac{R_0}{Q_0}Q$ of these modes.

I. INTRODUCTION

In Cornell's proposed Energy Recovery Linac, superconducting radio-frequency cavities with a fundamental frequency of 1.3 GHz will accelerate an electron beam to 5 GeV. The beam will excite higher-order modes (HOMs) that will drain power from the beam and kick it transversely. Because cavities will be held at 1.8 K, the cryogenic costs of dissipated power in the cavity will be high. In order to damp the HOMs and prevent HOM power from dissipating in the cavities, HOM loads that contain lossy materials will be positioned in the beam tube between cavities and held at 80 K. [1]

Two main figures of merit, Q and R_0/Q_0, will be used to characterize cavity-load systems in this paper. Q is defined as follows. [2]

$$Q = \frac{\omega_n U}{P_{diss}} \tag{1}$$

Q refers to the total quality factor of a mode and Q_0 to its quality factor from wall losses. ω_n of a mode equals $2\pi f$, U equals stored energy, and P_{diss} equals total dissipated power. R_0/Q_0, the shunt impedance, is defined as follows for monopole modes and dipole modes: [2]

$$(\frac{R_0}{Q_0})_{mon} = \frac{V_c^2}{2w_n U} \tag{2}$$

$$(\frac{R_0}{Q_0})_{dip} = \frac{\left|V_{||}(a)\right|^2}{2w_n U a^2} \tag{3}$$

V_c is the accelerating voltage on-axis and $V_{||}$ is the transverse voltage at a radial distance a from the cavity's axis. For modes with frequencies that are integer multiples of the bunch repetition frequency, resonant excitation can cause a high power transfer from the beam to the mode: $P = 2I^2\frac{R_0}{Q_0}Q$. Therefore, lowering $\frac{R_0}{Q_0}$ lowers the loss factor for monopole modes and lowering Q lowers the power loss for resonant modes. In addition, for dipole modes in ERLs, the threshold current for beam breakup is inversely proportional to $\frac{R_0}{Q_0}Q$.[3] Therefore, in order to reduce power losses and preserve beam stability, it is desirable to reduce $\frac{R_0}{Q_0}$ and Q of both monopole and dipole higher-order modes.

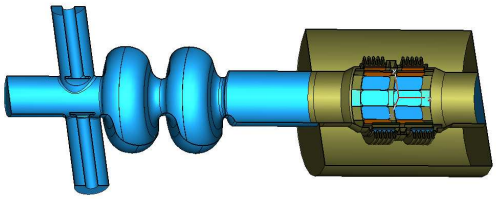

FIG. 1: CST MWS model of two-cell cavity and baseline 106 mm HOM load.

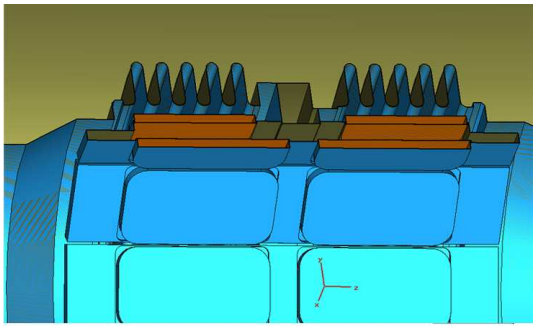

FIG. 2: Closeup of HOM load.

In this study, a HOM load was modeled with computer codes, then several parameters of its design were varied and the effects of the variations on $\frac{R_0}{Q_0}Q$ of the fundamental and higher-order modes were analyzed. Because the calculations using these models are extremely time-consuming, and the time required increases sharply with increased complexity of a model, it would be infeasible to do a full optimization of all these parameters on the HOM load with the full 7-cell cavity. Therefore, these optimizations were conducted using a simplified, 2-cell version of the cavity attached to the HOM load. Though this could not yield precise optimum points for the design of the load to be used with the full cavity, it showed how and how strongly different parameters affect $\frac{R_0}{Q_0}Q$ and how they affect different HOMs differently. This information will be allow the final optimization with the 7-cell cavity to be restricted to changes that have the potential to be useful in reducing $\frac{R_0}{Q_0}Q$, thereby reducing the required computing time to a feasible level.

II. TOOLS AND METHODS

A. CST Microwave Studio

CST Microwave Studio is a 3-D program that calculates eigenmodes of cavities in the presence of lossy materials. [4] Calculations are very time-consuming, so extensive optimizations in CST MWS are impractical.

A 3-D model of a baseline two-cell ERL injector cavity [5] and 106 mm diameter HOM load [6] was created in CST MWS (Fig. 1). The load contains 12 copper-covered metal plates, each of which has two lossy plates mounted on it, four made of each of TT2-111R ferrite, Co2Z ferrite or Ceralloy 137ZR10. [6] (Fig. 2) This model is set up such that its eigenmodes can be calculated at any time.

A CST MWS model was also made of a identical cavity and simplified load that did not include the bellows and that approximated the plates of ferrites and ceramics with four hollow cylinders mounted on a ring of metal. (Fig. 3, Fig. 4) One version of this model was made in which the cylinders were non-lossy, one in which they were made of the Ceralloy, one in which they were made of the TT2 ferrites, and one in which they were made of the Co2Z ferrite. These models are also set up such that their eigenmodes can be calculated at any time.

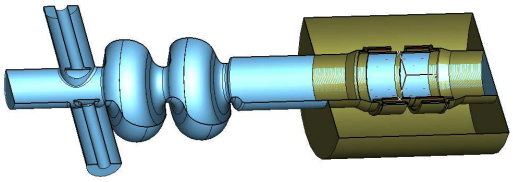

FIG. 3: CST MWS model of two-cell cavity and simplified 106 mm HOM load.

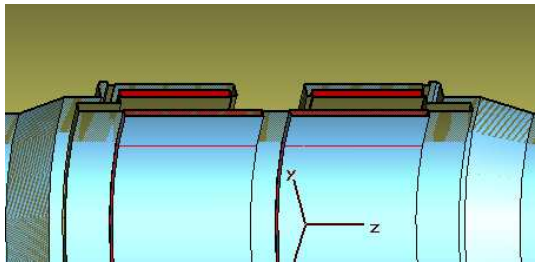

FIG. 4: Closeup of simplified load.

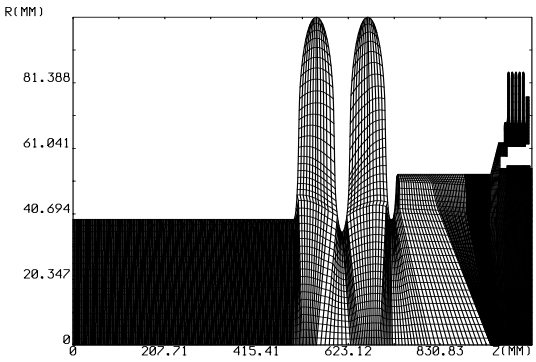

FIG. 5: Mesh of baseline cavity and half-load model in CLANS.

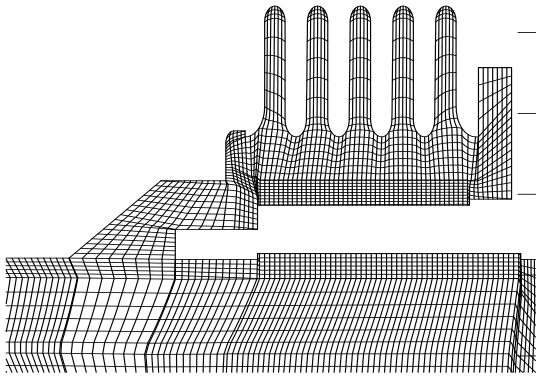

FIG. 6: Closeup of mesh around ferrites and metal plate in CLANS.

B. CLANS/CLANS2

CLANS is a 2-D computer code that calculates monopole modes of axially symmetric cavities with partial fillings of lossy dielectric materials, and CLANS2 is an analogous code for multipole modes.[7, 8] These programs were used to calculate the monopole modes of model loads with various design parameters, and programs to calculate dipole modes were created and are ready to be run.

Because the real baseline HOM load is axially asymmetric, 2-D codes cannot perfectly simulate it. Therefore, a CLANS model was created of a modified baseline two-cell cavity and HOM half-load in which hollow cylinders of lossy materials were substituted for the plates in the real baseline, as in the simplified CST MWS model.(Fig. 5, Fig. 6)[1] The tube on the opposite side of the cavity from the HOM load was of an arbitrary length. Due to time constraints, the TT2 ferrite was used as the lossy material in all optimizations, though in the real baseline HOM load the Co2Z ferrite and the Ceralloy are also present. Then, for each parameter in the optimization, a Matlab script was written to incrementally modify the geometry and the mesh of the baseline, to run CLANS, and to compile the relevant output. The CLANS models and routines were made first, and then for CLANS2, curves of radius 0.025 mm were incorporated to accomodate CLANS2's requirement that models have no sharp edges.[9]

[1] In CLANS figures in this paper, the scales of the x and y axes are different from each other and from the scales in other figures.

TABLE I: The four main parameters of the optimization and the limits and interval of their variation.

Parameter	Baseline (mm)	Change from Baseline (mm)	Interval (mm)
Tube Length	209.91	0 to 30.00	2.00
Ferrite Length	40.52/50.65[b]	0 to 30.00	2.00
Ferrite Thickness	3.17	-3.00 to 2.50	0.50
Ferrite Radius	54.06[c]	-30.00 to 2.00	2.00

[b]Outer ferrite/Inner ferrite
[c]Inner radius of inner ferrite

In each model, variations of four main parameters were tested: length of the tube between the cavity and the load, length of the ferrite plates (and of the entire load, to accomodate the ferrites), thickness of the ferrite plates, and radial distance of the metal plates and ferrites from the center of the load. (Table I) For each parameter, two Matlab routines each were written for CLANS and CLANS2, one with an odd and one with an even boundary condition at the edge of the half-load. Of these, all of the CLANS routines were run and the ferrite-thickening and tube-lengthening routines in CLANS2 were run. Due to time constraints, only CLANS routines with odd boundary conditions were analyzed, although CLANS routines with even load boundary conditions appeared to behave similarly in preliminary analysis. In addition, one model was made in which the inner ferrite was split into four parts, and all combinations of three possible heights for each ferrite were calculated; this model was run only in CLANS and only with an odd boundary condition. In each optimization, 27 to 42 modes were calculated for each model. Many of these modes had very low Q and were therefore not of concern. Analysis was done on the three to seven modes per model with Q greater than 1000.

III. RESULTS

In each optimization in the CLANS models, some subset of the monopole modes with frequencies close to 2957, 2999, 3068, 3160, 3270, 3388, and 3483 MHz had Q greater than 1000, so these were the HOMs studied. (Fig. 7) These modes had wavelengths ranging from about 88 to 101 mm. In each mode, the field was concentrated in the tube across the cavity from the half-load, and the magnetic field was roughly sinusiodal along the outer radius of this part of the tube.

In general, losses were not evenly distributed within the ferrites. The inner ferrite caused more losses than the outer ferrite, and the half of each ferrite closer to the cavity caused more losses than the other half. In one model close to the baseline, 61 percent of the losses were in the half of the inner ferrite that was closer to the cavity and 25 percent were in the half of the outer ferrite closer to the cavity. (Fig. 8)

Tube Length: Varying the length of the tube between the cavity and the load affected each high-Q HOM differently. (Fig. 9) $\frac{R_0}{Q_0}Q$ of HOMs appeared to have a sinusoidal dependence on tube length, with variation in $\frac{R_0}{Q_0}Q$ of about 30 percent or less per mode. About 1/3 of the sine functions's wavelength appeared over the 30 mm change, so the sine functions'

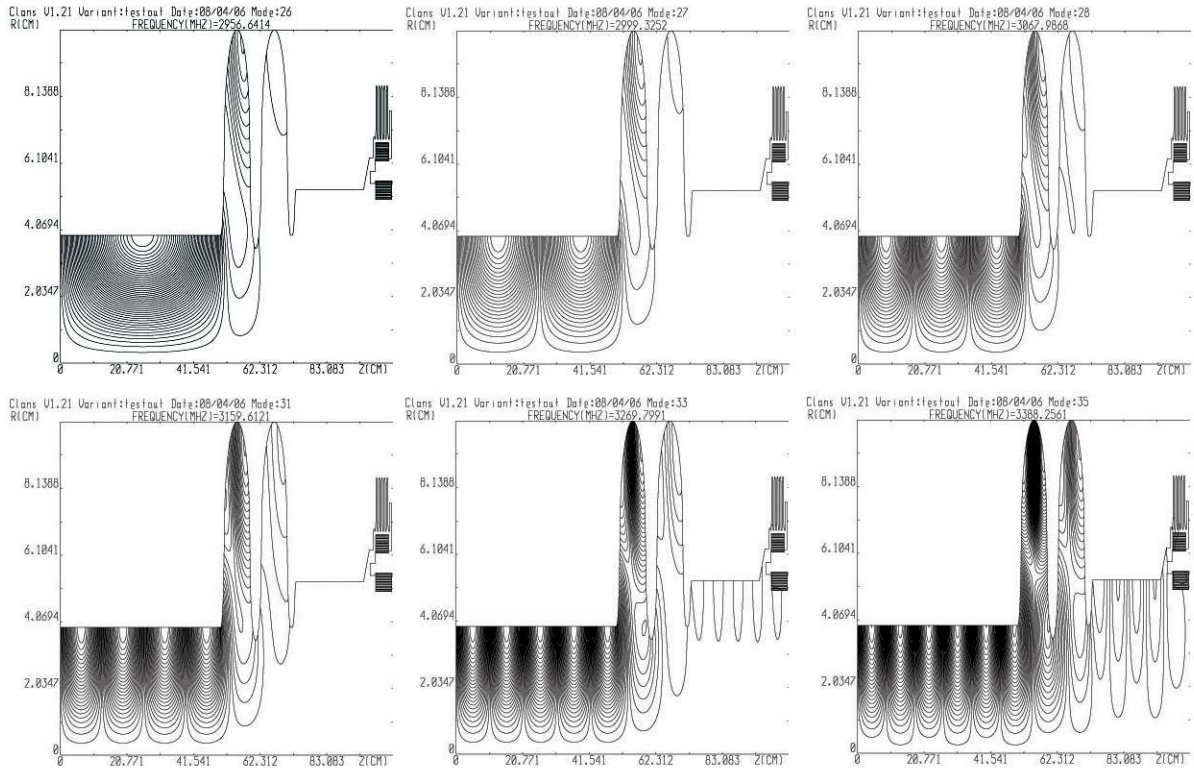

FIG. 7: Some HOMs with $Q > 1000$ in the models tested. First row: 2957 MHz, 2999 MHz, 3068 MHz. Second row: 3160 MHz, 3270 MHz, 3388 MHz.

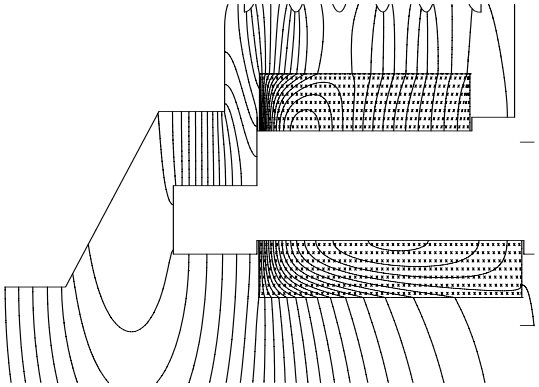

FIG. 8: Lines of equal magnetic field in an HOM. The majority of losses occur in the half of the lower ferrite closest to the cavity.

wavelengths were about 90 mm, which is comparable to the wavelengths of the HOMs. This dependence may have been caused by coupling between the cavity and the tube. As the tube was lengthened, its eigenmodes changed, and when one of them was close to a mode in the cavity, they may have coupled more strongly, which created higher fields and higher $\frac{R_0}{Q_0}Q$.

Ferrite Length: $\frac{R_0}{Q_0}Q$ also appeared to have a somewhat sinusoidal dependence on ferrite length, although it was damped with increasing ferrite length. (Fig. 10) Because of the

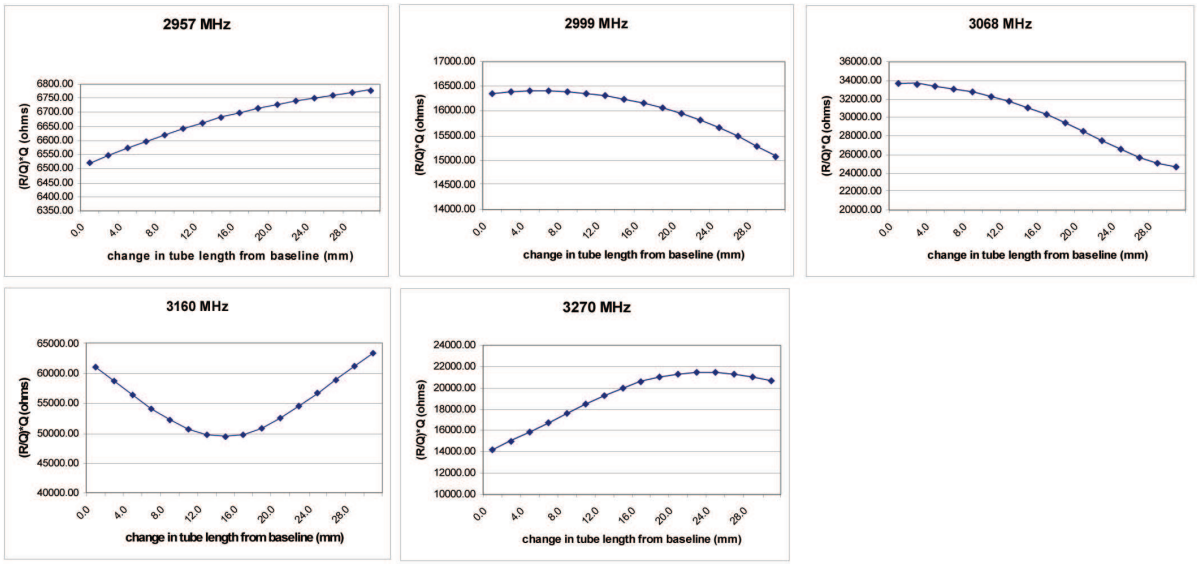

FIG. 9: $\frac{R_0}{Q_0}Q$ of high-Q monopole modes with varying length of tube between cavity and load from baseline of 209.91 mm.

structural changes necessary to lengthen the ferrites, the tube was also effectively lengthened, as in the previous optimization. Therefore, coupling between the cavity and the tube may have also caused the sinusoidal dependence in this case. Ferrite length changes had only a weak effect on losses, causing variations of about 10 percent or less in $\frac{R_0}{Q_0}Q$ with a ferrite length change of 60 percent. It seems that lengthening the ferrite is of limited benefit, possibly because the majority of the losses are in the part of the ferrite closest to the cavity.

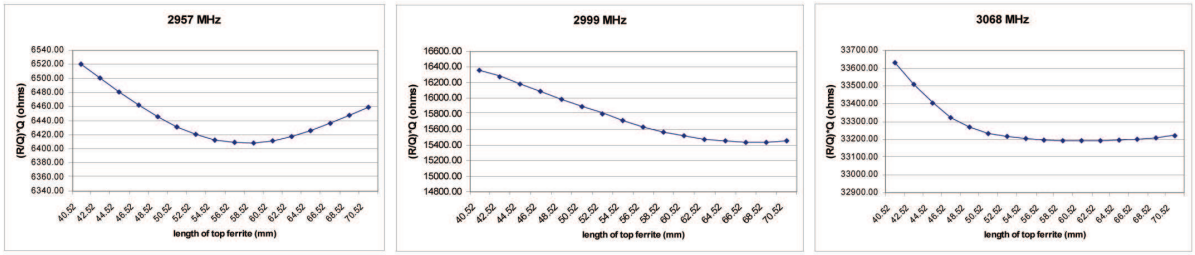

FIG. 10: $\frac{R_0}{Q_0}Q$ of high-Q monopole modes with varying ferrite length from baseline of 40.52/50.65 mm for the outer/inner ferrite.

Ferrite Thickness: Of the parameter changes performed, changing the thickness of the ferrite had the most dramatic effect on $\frac{R_0}{Q_0}Q$, with variations of up to about 85 percent from the maximum. (Fig. 11) Effects were different on different modes, but for several modes, $\frac{R_0}{Q_0}Q$ was very high for the thinnest ferrite, dropped sharply as it thickened, and then reached a point after which further thickening either reduced $\frac{R_0}{Q_0}Q$ very little or increased it slightly. If modes that behave like this dominate cause the majority of power loss to HOMs, then the examination of many modes of the final cavity could likely yield an optimum point. This behavior may be caused by resonance if a mode in the cavity or tube couples to a mode in the ferrite.

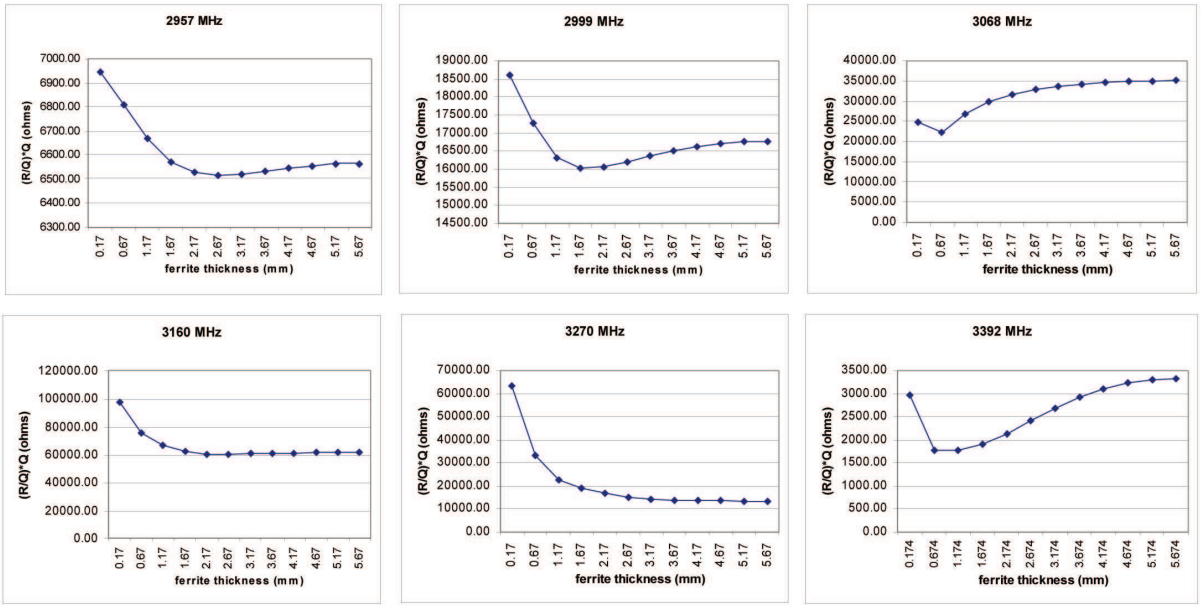

FIG. 11: $\frac{R_0}{Q_0}Q$ of high-Q monopole modes with varying ferrite thickness from baseline of 3.17 mm.

Radial Position: Changing the radial position of the ferrites also had a strong effect on some HOMs, reducing $\frac{R_0}{Q_0}Q$ by up to 78 percent from the maximum. (Fig. 12) The effects are markedly different for each HOM. In order to understand the differences, the absolute value of the real part of the magnetic field was calculated along a line from the central axis of the load into the inner ferrite. For each mode, $|Re(H)|$ was zero at the axis and the metal plate on which the ferrites were mounted, reached a maximum somewhere in between, and changed sharply going into the ferrite. For modes of frequency 2957, 2999, 3067, 3270, and 3388 MHz, each of which has a noticeable cluster of lower values of $\frac{R_0}{Q_0}Q$ with a minimum, this change in $|Re(H)|$ was negative. For modes of frequency 3160 and 3484, each of which has a cluster of higher values of $\frac{R_0}{Q_0}Q$ with a maximum, this change in $|Re(H)|$ was positive. This behavior is complex and not well understood, it may be caused by resonance of certain modes in the ferrites.

Split Ferrite: In the split lower ferrite model in which the four ferrites were the same thickness as the ferrites in the baseline model, the Qs for the tested high-Q modes were within 6 percent of the Q values of those modes in the baseline. (Table II) This indicates that losses depend more strongly on volume of the ferrites than on surface area. It was also found that losses are differently distributed between the parts of the ferrite for different models.

IV. CONCLUSIONS

The modes examined in the CLANS model are not the modes that will appear in the actual 7-cell cavity and load, for several reasons: the plates of ferrites are approximated by hollow cylinders; the modes depend on the length of the tube on the side of the cavity opposite the load, which is of an arbitrary length; the cavity used is a two-cell design, not

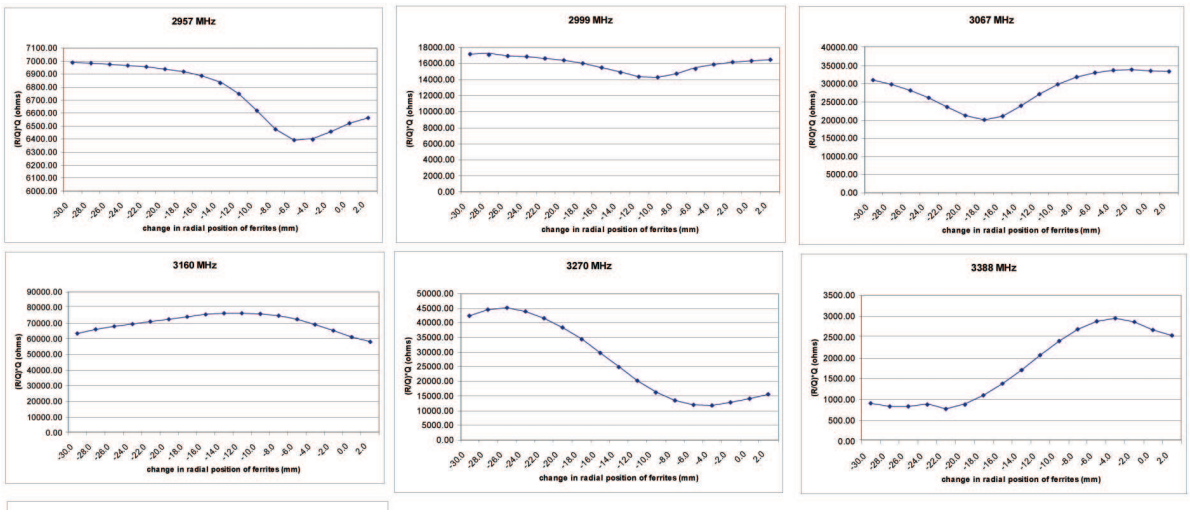

FIG. 12: $\frac{R_0}{Q_0}Q$ of high-Q monopole modes with varying radial position of ferrites and metal plate from baseline of 54.06 mm inner radius of inner ferrite.

TABLE II: Comparison of Q modes for the baseline and for the split ferrite model with the same ferrite thickness as the baseline.

Mode Frequency (MHz)	$\frac{R_0}{Q_0}Q$ Single Ferrite	Four Ferrites	Percent Change
2957	6520	6494	0.40
2999	16358	16186	1.05
3068	33633	33102	1.58
3160	61126	62389	-2.07
3270	14230	14355	-0.88
3392	2678	2529	5.55

a final optimized 7-cell design; and there is only one half-load, instead of a full load on each side. Also, many more modes than calculated will affect the power losses to HOMs, so any final optimization will have to involve the calculation of many more modes, in addition to compensating for the increase in the density of modes in frequency due to coupling between the cells in the longer cavity. However, calculating more modes and adding another load dramatically increases computing time, and doing a full study of many load design changes in a more complete model would be prohibitively time-consuming. The tests run in a final optimization must be chosen very carefully to use computing time efficiently. The optimizations done in this study, though they did not yield specific optimum points for parameters in the final model, found the types of effects that various design changes could have, and will give direction to future studies in choosing which parameters to optimize in order to achieve specific effects, and showing them what kind of side effects they might expect from these changes.

The radial position of the ferrites and the thickness of the ferrites were shown to substantially influence the damping of HOMs, and ferrite thickness in particular shows promise as a parameter that may have a clear optimum in a final design. Changing the distance

between the cavity and the load and changing the length of the ferrites were shown to be less influential, and the cost of increasing the distance between elements in the beam tube may outweigh the benefits of changing these parameters from the baseline.

Future study will be necessary to optimize the design of the HOM load. The runs done here with the TT2 ferrite may be repeated with the Ceralloy, the Co2Z ferrite, or combinations of the three. Using the CLANS2 routines written for this study, the effects of parameter changes on multipole modes can be explored, and eventually the routines may be combined to explore the effects of multiple parameter changes at once. The optimized 7-cell cavity with two full loads may be created and specific optimized values of the parameters for it determined. The Microwave Studio models may also be run, and their results compared to those of the CLANS models. In all of these possible objects of study, the amount of computing time required severely limits the rate of data acquisition, so care in the choice of models to be tested will improve the set of parameters chosen for the final design.

V. ACKNOWLEDGMENTS

I would like to thank Matthias Liepe and Valery Shemelin of Cornell University for their help and guidance, and Rich Galik for organizing the REU program. This work was supported by the National Science Foundation REU grant PHY-0552386 and research cooperative agreement PHY-0202078.

---

[1] M. Liepe, "Conceptual Layout of the Cavity String of the the Cornell ERL Main Linac Cryomodule", *Proceedings of 11th Workshop of RF Superconductivity*, Travemnde, Germany, September 8-12, (2003).

[2] H. Padamsee, J. Knobloch and T. Hays, *RF Superconductivity for Accelerators*, New York, John Wiley and Sons, (1998).

[3] G. Hoffstaetter and I. Bazarov, "Beam-breakup instability theory for energy recovery linacs", *Phys. Rev. ST Accel Beams*, **7** 054401 (2004).

[4] Computer Simulation Technology, "CST Microwave Studio", http://www.cst.com/Content/Products/MWS/Overview.aspx, (2006).

[5] V. Shemelin, H. Padamsee, and S. Belomestnykh, "Diople-mode-free and kick-free 2-cell cavity for the SC ERL Injector", *Proceedings of the 2003 Particle Accelerator Conference*, Portland, pp 2059-2061.

[6] V. Shemelin et al., "Status of HOM load for the Cornell ERL Injector", *Proceedings of the 2006 European Particle Accelerator Conference*, Edinburgh, (2006) (to be published).

[7] D.G. Myakishev and V.P. Yakovlev, "The New Possibilities of Superlans Code for Evaluation of Axisymmetric Cavities", *Proceedings of the 1995 Particle Accelerator Conference and International Conference on High-Energy Accelerators*, Dallas, TX, May 1995, Vol. 4, pp. 2348-2350.

[8] D.G. Myakishev, "CLANS2-A Code for Calculation of Multipole Modes in Axisymmetric Cavities with Absorber Ferrites", *Proceedings of the 1999 Particle Accelerator Conference*, New York, 1999, pp 2775-2777.

[9] R. Paryl,"CLANS2 Companion for a PC running Windows NT," Laboratory of Nuclear Studies, Cornell University, (1998).